

# Perifosine, an oral bioactive novel alkylphospholipid, inhibits Akt and induces in vitro and in vivo cytotoxicity in human multiple myeloma cells

Teru Hideshima, Laurence Catley, Hiroshi Yasui, Kenji Ishitsuka, Noopur Raje, Constantine Mitsiades, Klaus Podar, Nikhil C. Munshi, Dharminder Chauhan, Paul G. Richardson, and Kenneth C. Anderson

**Perifosine is a synthetic novel alkylphospholipid, a new class of antitumor agents which targets cell membranes and inhibits Akt activation. Here we show that baseline phosphorylation of Akt in multiple myeloma (MM) cells is completely inhibited by perifosine [octadecyl-(1,1-dimethyl-piperidino-4-yl)-phosphate] in a time- and dose-dependent fashion, without inhibiting phosphoinositide-dependent protein kinase 1 phosphorylation. Perifosine induces significant cytotoxicity in both MM cell lines and patient MM cells resistant to conventional therapeutic agents. Perifosine does not induce cytotoxicity in peripheral blood mono-**

**nuclear cells. Neither exogenous interleukin-6 (IL-6) nor insulinlike growth factor 1 (IGF-1) overcomes Perifosine-induced cytotoxicity. Importantly, Perifosine induces apoptosis even of MM cells adherent to bone marrow stromal cells. Perifosine triggers c-Jun N-terminal kinase (JNK) activation, followed by caspase-8/9 and poly (ADP)-ribose polymerase cleavage. Inhibition of JNK abrogates perifosine-induced cytotoxicity, suggesting that JNK plays an essential role in perifosine-induced apoptosis. Interestingly, phosphorylation of extracellular signal-related kinase (ERK) is increased by perifosine; conversely, MEK inhibitor syn-**

**ergistically enhances Perifosine-induced cytotoxicity in MM cells. Furthermore, perifosine augments dexamethasone, doxorubicin, melphalan, and bortezomib-induced MM cell cytotoxicity. Finally, perifosine demonstrates significant antitumor activity in a human plasmacytoma mouse model, associated with down-regulation of Akt phosphorylation in tumor cells. Taken together, our data provide the rationale for clinical trials of perifosine to improve patient outcome in MM. (Blood. 2006;107:4053-4062)**

© 2006 by The American Society of Hematology

## Introduction

Multiple myeloma (MM) is characterized by excess bone marrow (BM) plasma cells in association with monoclonal proteins. Despite conventional therapies with alkylating agents, anthracyclines, and corticosteroids,<sup>1,2</sup> as well as high-dose therapy and stem cell transplantation,<sup>3,4</sup> it remains incurable due both to intrinsic and acquired drug resistance.<sup>5-7</sup> Importantly, the BM microenvironment induces growth, survival, and drug resistance in MM cells via at least 2 different mechanisms: adhesion of MM cells to fibronectin confers cell adhesion-mediated drug resistance (CAM-DR)<sup>8,9</sup>; and cytokines (ie, interleukin-6 [IL-6], insulinlike growth factor 1 [IGF-1], and vascular endothelial growth factor [VEGF]) in the BM milieu induce mitogen-activated protein kinase (MAPK) kinase (MEK)/extracellular signal-related kinase (ERK); phosphatidylinositol 3-kinase (PI3-K)/Akt; and/or Janus kinase 2 (JAK2)/signal transducer activator of transcription 3 (STAT3) signaling cascades. Akt signaling mediates MM cell resistance to conventional therapeutics<sup>10-14</sup>; therefore, biologically based treatments targeting Akt may induce anti-MM activity in the context of the BM microenvironment.

Perifosine [octadecyl-(1,1-dimethyl-piperidino-4-yl)-phosphate] is a synthetic novel alkylphospholipid (ALP), a new class of antitumor agents which targets cell membranes, inhibits Akt

activation, and induces apoptosis in PC-3 prostate carcinoma cells,<sup>15</sup> epithelial carcinoma cell line A431, and HeLa cells.<sup>16</sup> Importantly, perifosine does not directly affect activity of PI3-K or phosphoinositide-dependent kinase 1 (PDK1).<sup>15</sup> It induces p21<sup>Cip1</sup>, associated with G<sub>2</sub>/M phase cell accumulation, in head and neck squamous cell carcinoma cells.<sup>17</sup> p21<sup>Cip1</sup> induction is due to activation of ERK signaling pathway by perifosine, since ERK activation promotes the phosphorylation of Sp1 in known ERK threonine residues (Thr 453/739), thereby leading to increased Sp1 binding and enhanced p21<sup>Cip1</sup> transcription.<sup>18</sup> Most recently, combination treatment of human leukemia cells with perifosine and histone deacetylase inhibitors (HDACs) inhibited both Akt and MEK/ERK, induced ceramide and reactive oxygen species production and mitochondrial injury, and triggered apoptosis.<sup>19</sup> In 2 phase 1 studies of perifosine in solid tumors, dose-limiting toxicity (DLT) was not reached, although gastrointestinal toxicity led to early treatment discontinuation at higher dose levels. Importantly, no hematologic toxicity was observed, and maximum-tolerated dose (MTD) was defined at 200 mg/d, achieving plasma concentrations of perifosine of 7.5 μg/mL (16.2 μM).<sup>20</sup>

In this report, we demonstrate that perifosine induces potent cytotoxicity associated with significant inhibition of Akt activity in

From the Jerome Lipper Multiple Myeloma Center, Department of Medical Oncology, Dana-Farber Cancer Institute and Boston Veterans Administration (VA) Healthcare System, Harvard Medical School, Boston, MA.

Submitted August 24, 2005; accepted January 4, 2005. Prepublished online as *Blood* First Edition Paper, January 17, 2006; DOI 10.1182/blood-2005-08-3434.

Supported by National Institutes of Health (NIH) SPORE IP50 CA10070, PO-1 78378, and RO-1 CA 50947 grants; the Doris Duke Distinguished Clinical Research Scientist Award (K.C.A.); the Multiple Myeloma Research

Foundation (T.H.); and the Cure for Myeloma Research Fund (K.C.A.).

T.H. and L.C. contributed equally to this work.

**Reprints:** Kenneth C. Anderson, Dana-Farber Cancer Institute, Mayer 557, 44 Binney St, Boston, MA 02115; e-mail: kenneth\_anderson@dfci.harvard.edu.

The publication costs of this article were defrayed in part by page charge payment. Therefore, and solely to indicate this fact, this article is hereby marked "advertisement" in accordance with 18 U.S.C. section 1734.

© 2006 by The American Society of Hematology

MM cell lines, as well as freshly isolated patient MM cells (inhibitory concentration at 50% [IC<sub>50</sub>] of 1.5–15  $\mu$ M at 48 hours). MM cell apoptosis triggered by perifosine is mediated via caspase-8, caspase-9, and poly(ADP-ribose) polymerase (PARP) cleavage, common apoptotic pathways in MM.<sup>13</sup> As with the proteasome inhibitor bortezomib<sup>21</sup> and immunomodulatory derivatives of thalidomide (IMiDs),<sup>22</sup> Perifosine augments dexamethasone (Dex)-induced MM cell growth inhibition; it also augments doxorubicin (Dox), melphalan (Mel), and bortezomib-induced MM cell cytotoxicity. IL-6<sup>10,11,23–26</sup> and IGF-1<sup>27,28</sup> induce MM cell growth and protection against Dex-induced apoptosis; however, neither exogenous IL-6 nor IGF-1 overcomes perifosine-induced cytotoxicity. Adherence of MM cells to bone marrow stromal cells (BMSCs) augments MM cell growth and protects against Dex-induced apoptosis,<sup>11,29</sup> but perifosine induces apoptosis even of MM cells adherent to BMSCs. Finally, perifosine inhibits human MM cell growth and prolongs host survival in a murine model of human MM, associated with *in vivo* inhibition of Akt in tumor cells. Our data provide the framework for clinical trials of perifosine to improve patient outcome in MM.

## Materials and methods

### Cells

Dex-sensitive (MM.1S) and -resistant (MM.1R) human MM cell lines were kindly provided by Dr Steven Rosen (Northwestern University, Chicago, IL). RPMI8226 and U266 human MM cells were obtained from American Type Culture Collection (Rockville, MD). The INA-6 cell line was kindly provided by Dr Martin Gramatzki (University of Erlangen-Nuernberg, Erlangen, Germany). Melphalan-resistant RPMI-LR5 (LR5) and doxorubicin-resistant RPMI-Dox40 (Dox40) cell lines were provided by Dr William Dalton (H Lee Moffitt Cancer Center, Tampa, FL). OPM1 and OPM2 were provided from Dr P. Leif Bergsagel (Mayo Clinic, Tucson, AZ). All MM cell lines were cultured in RPMI-1640 containing 10% fetal bovine serum (FBS; Sigma Chemical, St Louis, MO), 2  $\mu$ M L-glutamine, 100 U/mL penicillin, and 100  $\mu$ g/mL streptomycin (GIBCO, Grand Island, NY).

Patient MM cells were purified from BM aspirates by negative selection (RosetteSep separation system; StemCell Technologies, Vancouver, BC, Canada). The purity of MM cells was confirmed by flow cytometric analysis using anti-CD138 Ab (BD Pharmingen, San Diego, CA), as in prior studies.<sup>30</sup> Peripheral blood mononuclear cells (PBMCs) were obtained from healthy volunteers by Ficoll-Hipaque density sedimentation.

BM specimens were obtained from patients with MM. Mononuclear cells (MNCs) separated by Ficoll-Hipaque density sedimentation were used to establish long-term BM cultures, as in prior studies.<sup>29</sup> When an adherent cell monolayer had developed, cells were harvested in Hanks buffered saline solution containing 0.25% trypsin and 0.02% EDTA, washed, and collected by centrifugation. Approval for these studies was obtained from the Dana-Farber Cancer Institute Institutional Review Board. Informed consent was obtained from all patients in accordance with the Declaration of Helsinki protocol.

### Transfection

MM.1S cells were transfected with a plasmid vector carrying an Akt construct containing a myristoylation (Myr) site, leading to constitutive activation of Akt kinase (Upstate Biotechnologies, Lake Placid, NY), as in prior studies.<sup>12</sup> MM.1S cells were also transiently transfected with JNK2 $\alpha$ 2/SAPK1 $\alpha$  expression plasmid (Upstate Biotechnologies) using Nucleofector Kit V (Amaxa Biosystems, Cologne, Germany), as in prior studies.<sup>31</sup>

### Reagents

Perifosine (NSC 639966), a synthetic substituted heterocyclic alkylphospholipid, was provided by Keryx Biopharmaceuticals (New York, NY). Dex,

Dox, and Mel were purchased from Sigma Chemical. Bortezomib was obtained from Millennium Pharmaceuticals (Cambridge, MA). JNK inhibitor SP600215 and MEK1/2 inhibitor U0126 were purchased from Calbiochem (San Diego, CA) and Cell Signaling Technology (Beverly, MA), respectively. p38 MAPK inhibitor SCIO-469 was provided by Scios (Fremont, CA). Caspase-8 (Z-IETD-FMK), caspase-9 (Z-LEHD-FMK), and pancaspase (Z-VAD-FMK) inhibitors were purchased from Calbiochem.

### Growth inhibition assay

The inhibitory effect of perifosine, alone or combined with other agents, on MM cell growth was assessed by measuring 3-(4,5-dimethylthiazol-2-yl)-2,5-diphenyl tetrasodium bromide (MTT; Chemicon International, Temecula, CA) dye absorbance. Cells were pulsed with 10  $\mu$ L of 5 mg/mL MTT to each well for the last 4 hours of 24-hour and/or 48-hour cultures, followed by 100  $\mu$ L isopropanol containing 0.04 N HCl. Absorbance was measured at 570/630 nm using a spectrophotometer (Molecular Devices, Sunnyvale, CA).

### DNA synthesis

Proliferation was measured by DNA synthesis. MM cells ( $3 \times 10^4$  cells/well) were incubated in 96-well culture plates (Costar, Cambridge, MA) in the presence of media, perifosine, and/or other agents or recombinant cytokines (IL-6, IGF-1; R&D Systems, Minneapolis, MN) for 48 hours at 37°C. DNA synthesis was measured by [<sup>3</sup>H]-thymidine ([<sup>3</sup>H]-TdR; Perkin Elmer, Boston, MA) uptake. Cells were pulsed with [<sup>3</sup>H]TdR (0.0185 MBq/well [0.5  $\mu$ Ci/well]) during the last 8 hours of 48-hour cultures. All experiments were performed in triplicate.

### Immunoblotting

MM cells were harvested and lysed using lysis buffer: 50 mM Tris-HCl (pH 7.4), 150 mM NaCl, 1% NP-40, 5 mM EDTA, 5 mM NaF, 2 mM Na<sub>3</sub>VO<sub>4</sub>, 1 mM PMSF, 5  $\mu$ g/mL leupeptine, and 5  $\mu$ g/mL aprotinin. Whole-cell lysates were subjected to sodium dodecyl sulfate-polyacrylamide gel electrophoresis (SDS-PAGE) and transferred to PVDF membrane (Bio-Rad Laboratories, Hercules, CA). The Abs used for immunoblotting included: anti-phospho (p)-Akt (Ser473), anti-p-Akt (Thr308), anti-Akt, anti-p-PDK1 (Ser241), anti-p-FKHR (Thr24)/FKHRL1 (Thr32), anti-p-GSK3 $\alpha$ / $\beta$  (Ser21/9), anti-p-MEK (Ser217/221), anti-p-SAPK/JNK (Thr183/Tyr185), anti-SAPK, anti-caspase-8, anti-caspase-9, and anti-PARP (Cell Signaling Technology); as well as anti-p-ERK (Tyr204), anti-ERK1/2, anti-ERK2, anti-p-STAT3 (Tyr705), anti-JNK2, and anti- $\alpha$ -tubulin (Santa Cruz Biotechnology, Santa Cruz, CA) antibodies (Abs).

### In vitro Akt kinase assay

MM.1S cells were cultured in the presence or absence of perifosine (5  $\mu$ M, 6 hours) and then stimulated with IL-6 (20 ng/mL, 10 minutes). *In vitro* Akt kinase assay was then carried out using the Akt Kinase Assay Kit (nonradioactive) (Cell Signaling Technology).

### Flow cytometric analysis

For cell-cycle analysis, MM cells cultured for 24 hours in perifosine or control media were harvested, washed with phosphate-buffered saline (PBS), fixed with 70% ethanol, and treated with 10  $\mu$ g/mL RNase (Roche Diagnostics, Indianapolis, IN). Cells were then stained with propidium iodide (PI; Sigma Chemical) (5  $\mu$ g/mL) and the cell-cycle profile was determined using an Epics (Coulter Immunology, Hialeah, FL) flow cytometer, as in prior studies.<sup>32</sup>

### Effect of perifosine on paracrine MM cell growth in the BM

To evaluate growth stimulation and signaling in MM cells adherent to BMSCs,  $3 \times 10^4$  MM.1S cells were cultured in BMSC-coated 96-well plates for 48 hours in the presence or absence of perifosine. DNA synthesis was measured as described in "DNA synthesis."

**Xenograft murine model**

Beige-nude-xid (BNX) mice (5 to 6 weeks old) were obtained from Frederick Cancer Research and Development Center (Frederick, MD). All animal studies were conducted according to protocols approved by the Animal Ethics Committee of the Dana-Farber Cancer Institute. The mice were inoculated subcutaneously in the right flank with  $3 \times 10^7$  MM.1S MM cells in 100  $\mu$ L RPMI 1640 and 100  $\mu$ L Matrigel basement membrane matrix (Becton Dickinson, Bedford, MA). When tumors were measurable, mice were assigned into cohorts receiving oral perifosine daily (36 mg/kg) or weekly (250 mg/kg), or into a control group receiving oral vehicle alone (0.9% sodium chloride). The weekly dose was given in 2 divided doses (125 mg/kg/100  $\mu$ L PBS) to improve tolerance. Caliper measurements of the longest perpendicular tumor diameters were performed every alternate day to estimate the tumor volume, using the following formula representing the 3-dimensional volume of an ellipse:  $4/3 \times (\text{width}/2)^2 \times (\text{length}/2)$ . Animals were killed when tumors reached 2 cm or if the mice appeared moribund to prevent unnecessary morbidity to the mice. Survival was evaluated from the first day of treatment until death. Tumor growth was evaluated using caliper measurements from the first day of treatment until day of first killing which was day 15 for controls, day 32 for daily treated mice, and day 30 for weekly treated mice. Serum paraprotein was not detectable by enzyme-linked immunosorbent assay in this xenograft model.

**Statistical analysis**

Statistical significance of differences observed in drug-treated versus control cultures was determined using the Wilcoxon signed ranks test. The

minimal level of significance was a *P* value less than .05. The interaction between perifosine and bortezomib was analyzed by isobologram analysis using the CalcuSyn software program (Biosoft, Ferguson, MO) to determine whether the combination was additive or synergistic; a combination index (CI) lower than 0.7 indicates a synergistic effect, as previously described.<sup>32</sup> For in vivo experiments, tumor volumes were compared using 1-way analysis of variance and Bonferroni post hoc tests. Survival was assessed using Kaplan-Meier curves and log-rank analysis.

**Results**

**Perifosine inhibits Akt activation and induces cytotoxicity in MM cells**

We first examined baseline phosphorylation (Ser473) of Akt in 9 MM cell lines, including those resistant to conventional therapeutic agents (MM.1R, LR5, Dox40) and phosphatase tensin homolog (PTEN)-mutated (OPM1), as well as tumor cells from 3 MM patients. Five of 9 MM cell lines and 3 MM patient tumor cells demonstrated constitutive phosphorylation of Akt (Figure 1A). Interestingly, there was no relationship between Akt and STAT3 or ERK phosphorylation in these cells. Since previous studies demonstrated that perifosine inhibits Akt phosphorylation/activation in epithelial carcinoma cells (A431 and HeLa),<sup>16</sup> prostate carcinoma cells (PC-3),<sup>15</sup> lung adenocarcinoma cells (A549),<sup>33</sup> and leukemia

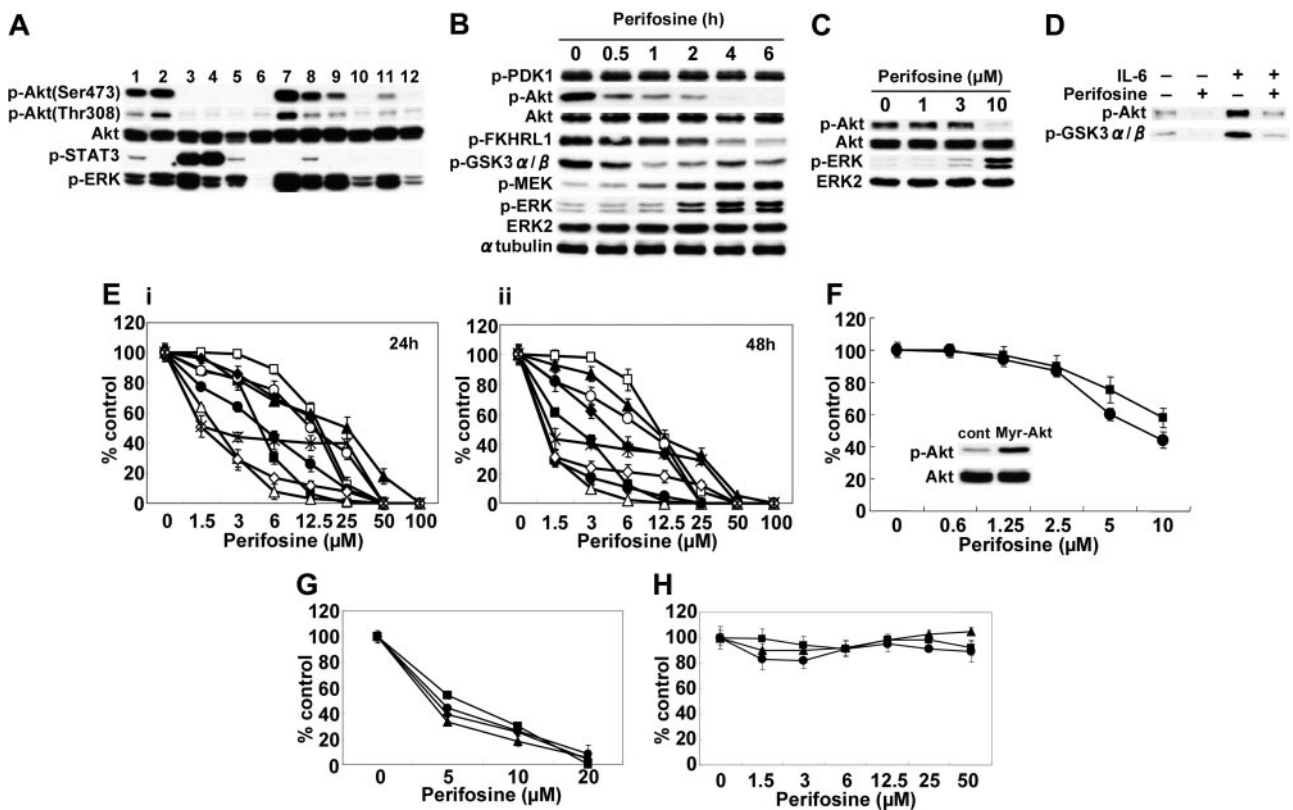


**Figure 1. Perifosine inhibits Akt phosphorylation and induces cytotoxicity in MM cells.** (A) Baseline phosphorylation of Akt, STAT3, and ERK in MM cell lines and tumor cells from MM patients assessed by Western blotting. Lane 1 indicates MM.1S; 2, MM.1R; 3, U266; 4, INA-6; 5, RPMI8226; 6, LR5; 7, Dox40; 8, OPM1; 9, OPM2; and 10 to 12, patient tumor cells. (B) MM.1S cells were cultured with perifosine (10  $\mu$ M) for the indicated periods. Whole-cell lysates were subjected to Western blotting using anti-p-PDK1, anti-p-Akt, anti-Akt, anti-p-FKHRL1, anti-p-GSK3 $\alpha/\beta$ , anti-p-MEK, anti-p-ERK, anti-ERK2, and  $\alpha$ -tubulin Abs. (C) MM.1S cells were cultured with perifosine (1-10  $\mu$ M) for 6 hours. Whole-cell lysates were subjected to Western blotting using anti-p-Akt, anti-Akt, anti-p-ERK, and anti-ERK2 Abs. (D) MM.1S cells were cultured with perifosine (5  $\mu$ M) for 6 hours prior to stimulation with IL-6 (20 ng/mL). Whole-cell lysates were immunoprecipitated with anti-Akt Ab. The immunoprecipitates were washed and subjected to in vitro kinase assay according to manufacturer's protocol. (E) MM.1S (■), MM.1R (□), U266 (▲), INA-6 (△), RPMI8226 (●), LR5 (○), Dox40 (◆), OPM1 (◇), and OPM2 (\*) cells were cultured with perifosine (1.5-100  $\mu$ M) for 24 hours (i) and 48 hours (ii). (F) MM.1S cells stably transfected with Myr-Akt (■) and control construct (●) were cultured with perifosine (0.6-10  $\mu$ M) for 24 hours. Whole-cell lysates from control and Myr-Akt-transfected cells were subjected to Western blotting using anti-p-Akt and Akt Abs. (G-H) Freshly isolated tumor cells from 4 patients with MM (G) and PBMCs from 3 healthy donors (H) were cultured with increasing doses of perifosine for 48 hours. Cytotoxicity was assessed by MTT assay (E-H); data represent mean ( $\pm$  SD) of quadruplicate cultures.

cells (U937 and HL60),<sup>19</sup> we next determined whether perifosine could inhibit Akt phosphorylation in MM cells. Whole-cell lysates from MM.1S cells cultured with 10  $\mu$ M perifosine for 0.5 to 6 hours were immunoblotted with p-Akt. MM.1S cells demonstrated constitutive phosphorylation of Akt, which was completely inhibited by perifosine in a time-dependent fashion (Figure 1B). Phosphorylation of FKHRL1 and GSK3 $\alpha/\beta$ , downstream target proteins of Akt, was also markedly inhibited; in contrast, phosphorylation of PDK-1, a known upstream molecule of Akt, was not affected by perifosine. Interestingly, phosphorylation of MEK and ERK was significantly increased by perifosine. This effect of perifosine on phosphorylation of Akt was dose dependent, with significant inhibition by 10  $\mu$ M perifosine for 6 hours (Figure 1C). These results demonstrate that perifosine inhibits baseline phosphorylation of Akt and its downstream target proteins without altering PDK1; conversely, perifosine enhances MEK and ERK phosphorylation. Similar results were observed in MM.1R and INA-6 cells (data not shown). In vitro Akt kinase assays confirmed the direct inhibitory effect of perifosine on Akt activity, before and after IL-6 stimulation of MM.1S cells; perifosine completely blocked both baseline and IL-6-stimulated phosphorylation of GSK3 $\alpha/\beta$  (Figure 1D). This result indicates that perifosine directly inhibits Akt activity, even in IL-6-stimulated MM cells.

We next examined the growth inhibitory effect of perifosine in MM cell lines using MTT assays. MM.1S, MM.1R, U266, INA-6, RPMI8226, RPMI-LR5, RPMI-Dox40, OPM1, and OPM2 cells were cultured for 24 hours (Figure 1E, left panel) and 48 hours (Figure 1E, right panel) in the presence of perifosine (1.5-100  $\mu$ M). Perifosine significantly inhibited growth of these cell lines at 48

hours in a dose-dependent fashion, with IC<sub>50</sub> of 1 to 12.5  $\mu$ M. We further examined whether perifosine could overcome constitutive highly active Akt in MM cells. To test this hypothesis, we used Myr-Akt-MM.1S cells stably transfected with Myr-Akt. Importantly, perifosine is also effective in these transfectants (Figure 1F). These results suggest that perifosine does not inhibit upstream molecules, but targets Akt. The cytotoxicity of perifosine was also assessed in freshly isolated tumor cells from MM patients (n = 4). Perifosine (5-20  $\mu$ M) induced significant anti-MM activity, with IC<sub>50</sub> as in MM cell lines (Figure 1G). In contrast, perifosine did not trigger cytotoxicity in PBMCs from 3 healthy volunteers (Figure 1H). These results demonstrate that perifosine triggers significant cytotoxicity even in drug-resistant (MM.1R, LR5, and Dox40) MM cell lines and patient MM cells, without toxicity in normal PBMCs.

### Perifosine induces JNK/caspase-dependent MM cell apoptosis

We next examined molecular mechanisms whereby perifosine induces cytotoxicity in MM cells. We first performed cell-cycle profiling using PI staining in MM.1S and RPMI8226 cells cultured for 24 hours with control media or perifosine (5  $\mu$ M and 10  $\mu$ M). perifosine induced increased sub-G<sub>1</sub> phase population in both MM.1S and RPMI8226 cells. For example, sub-G<sub>1</sub> phase MM.1S cells increased from 15% in control to 36% and 57% after treatment with 5  $\mu$ M and 10  $\mu$ M perifosine, respectively (Figure 2A). To determine whether perifosine-induced cytotoxicity is mediated via activation of caspase and/or PARP, MM.1S cells were treated with 5  $\mu$ M and 10  $\mu$ M for 8 hours; perifosine induced caspase-8, caspase-9, and PARP cleavage in a dose- and time-dependent fashion (Figure 2B). Similar results were observed in

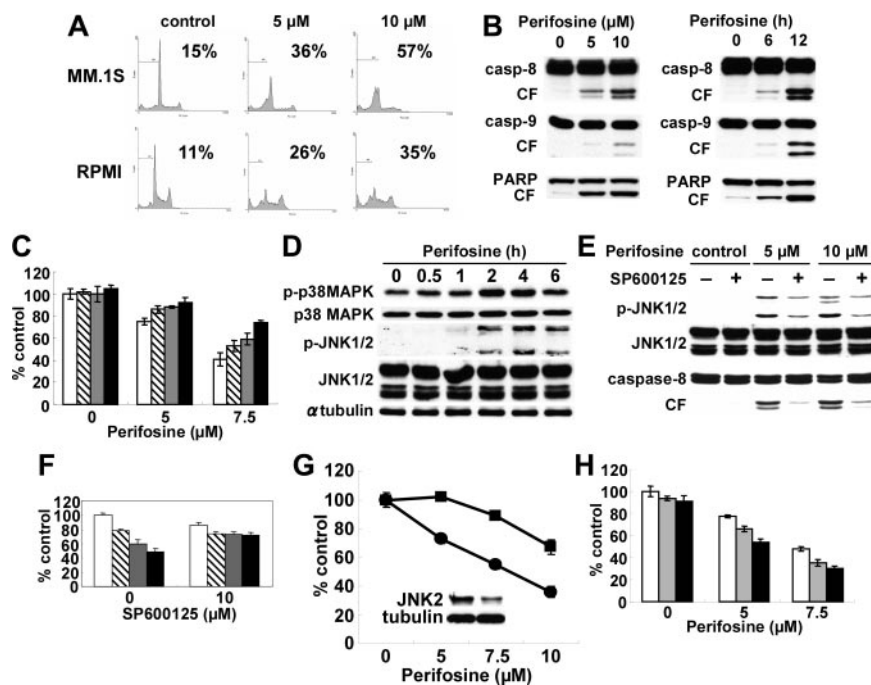


**Figure 2. Perifosine induces JNK/caspase-dependent MM cell apoptosis.** (A) MM.1S and RPMI8226 cells were cultured with perifosine (5 and 10  $\mu$ M) for 24 hours. Cells were then subjected to cell-cycle profiling by PI staining and flow cytometry. Percentage indicates sub-G<sub>1</sub> phase cells. (B) MM.1S cells were cultured with perifosine (5 and 10  $\mu$ M) for 8 hours. (C) MM.1S cells were also cultured with perifosine (10  $\mu$ M) for 6 and 12 hours. Cells were then lysed and subjected to Western blotting using caspase-8, caspase-9, and PARP Abs. (D) MM.1S cells were cultured for 24 hours with perifosine (5 and 7.5  $\mu$ M) in the presence of control media (□), and with 25  $\mu$ M of Z-IETD-FMK (▨), Z-LEHD-FMK (▩), or Z-VAD-FMK (■). (E) MM.1S cells were cultured with perifosine (5  $\mu$ M and 10  $\mu$ M) for 8 hours, in the presence or absence of SP600125 (10  $\mu$ M). Cells were then lysed and subjected to Western blotting using anti-p-JNK, anti-JNK, and caspase-8 Abs. (F) MM.1S cells were cultured for 24 hours with control media (□), or with 2.5  $\mu$ M (▨), 5  $\mu$ M (▩), and 7.5  $\mu$ M (■) perifosine, in the presence or absence of SP600126 (10  $\mu$ M). (G) MM.1S cells were transiently transfected with control (●) or JNK2 siRNA expression plasmid (■). Whole-cell lysates were subjected to Western blotting using anti-JNK2 and  $\alpha$ -tubulin Abs. (H) MM.1S cells were cultured for 24 hours with control media (□) or perifosine (5 and 7.5  $\mu$ M) in the presence or absence of control media (□), 200 nM (▨), or 400 nM (■) SCIO469. Cytotoxicity was assessed by MTT assay; data represent mean ( $\pm$  SD) of quadruplicate cultures.

RPMI8226 cells treated with perifosine (data not shown). To further examine whether caspase inhibitor could block perifosine-induced cytotoxicity, MM.1S cells were cultured with perifosine in the presence of Caspase-8 (Z-IETD-FMK), caspase-9 (Z-LEHD-FMK), and pan-caspase (Z-VAD-FMK) inhibitors. Importantly, these inhibitors significantly ( $P < .01$ ) reduced perifosine-induced cytotoxicity (Figure 2C). Taken together, these results strongly suggest that perifosine triggers caspase-dependent apoptosis in MM cells.

Since we have shown that JNK plays a crucial role in apoptosis triggered by novel therapeutic agents, including bortezomib<sup>30</sup> and lysophosphatidic acyltransferase inhibitor,<sup>34</sup> and Rahmani et al<sup>19</sup> have reported that perifosine induced phosphorylation of JNK in U937 cells, we next examined whether perifosine induced phosphorylation of JNK during MM cell apoptosis. As shown in Figure 2D, Perifosine strongly induced phosphorylation of JNK1/2 in MM.1S cells in a time-dependent fashion. Phosphorylation of p38 MAPK was also induced by perifosine treatment. To determine the role of JNK activity in mediating perifosine-induced cytotoxicity, MM.1S cells were treated with perifosine in the presence or absence of the JNK inhibitor SP600125.<sup>35,36</sup> SP600125 markedly inhibited perifosine-induced phosphorylation of JNK and caspase-8 cleavage (Figure 2E). Consistent with inhibition of perifosine-induced phosphorylation of JNK1/2 and caspase-8, cytotoxicity triggered by perifosine (5  $\mu$ M and 10  $\mu$ M for 8 hours) was blocked by SP600125 (Figure 2F), confirming that SP600125 inhibits perifosine-induced JNK activation and caspase-8 cleavage. Similar results were observed in RPMI8226 cells (data not shown). Previous studies have shown that JNK2 plays an important role in apoptosis<sup>37</sup>; we therefore further examined whether specific inhibition of JNK2 expression could block perifosine-induced cytotoxicity. MM.1S cells transfected with JNK2 shRNA expression plasmid significantly reduced perifosine-induced cytotoxicity ( $P < .01$ , control vector versus expression plasmid), associated with decreased JNK2 protein expression (Figure 2G). These results suggest that JNK plays a role, at least in part, mediating MM cell apoptosis triggered by perifosine.

We have previously shown that bortezomib induces phosphorylation/activation of p38 MAPK and that p38 MAPK inhibitor SCIO-469 augments its cytotoxicity.<sup>31</sup> Since perifosine triggered phosphorylation of p38 MAPK, we similarly examined whether SCIO-469 also enhances perifosine-induced cytotoxicity in MM cells. As expected, SCIO-469 augments perifosine-induced cytotoxicity in a dose-dependent fashion (Figure 2H). Our ongoing studies will delineate molecular mechanisms whereby inhibition of p38 MAPK enhances perifosine-induced cytotoxicity.

#### Neither growth factors nor adherence to BMSCs protect against perifosine-induced MM cell cytotoxicity

IL-6 triggers significant MM cell growth and antiapoptotic activities in vitro<sup>24,38,39</sup> and in vivo in murine models of human MM.<sup>40,41</sup> Specifically, we have demonstrated that IL-6 abrogates Dex-induced apoptosis via activation of Akt in MM.1S cells.<sup>11</sup> We next therefore examined whether IL-6 could overcome the antiapoptotic effect of perifosine in vitro. Consistent with our previous studies,<sup>11</sup> Dex-triggered MM cell cytotoxicity was almost completely abrogated by IL-6 (10 ng/mL); importantly, IL-6 did not block perifosine-triggered cytotoxicity (Figure 3A). Similar results were observed in the presence of IGF-1 (data not shown). The impact of perifosine on signaling cascades mediated by IL-6 and IGF-1 was further examined. MM.1S cells were incubated with perifosine (5  $\mu$ M for 6 hours), prior to stimulation with IL-6 (10 ng/mL) or IGF-1 (25 ng/mL). IL-6 induced phosphorylation of Akt, ERK and

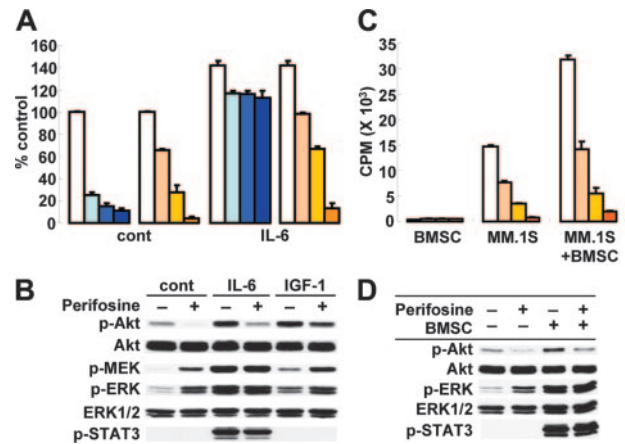


**Figure 3. Neither growth factors nor adherence to BMSCs protect against perifosine-induced MM cell cytotoxicity.** (A) MM.1S cells were cultured for 48h with control media (white bars); with 50 nM (light blue bars), 100 nM (medium blue bars), and 200 nM (dark blue bars) Dex; or with 2.5  $\mu$ M (light orange bars), 5  $\mu$ M (medium orange bars), and 10  $\mu$ M (dark orange bars) perifosine, in the presence or absence of IL-6 (10 ng/mL). Cytotoxicity was assessed by MTT assay; data represent means ( $\pm$  SD) of quadruplicate cultures. (B) MM.1S cells were cultured with control media or perifosine (5  $\mu$ M) for 6 hours. Cells were then stimulated with IL-6 (10 ng/mL) or IGF-1 (25 ng/mL) for 10 minutes. Whole-cell lysates were subjected to Western blotting using anti-p-Akt, anti-Akt, anti-p-MEK, anti-p-ERK, anti-ERK1/2, and p-STAT3 Abs. (C) MM.1S cells were cultured with control media (white bars); and with 1.25  $\mu$ M (light orange bars), 2.5  $\mu$ M (medium orange bars), and 5  $\mu$ M (dark orange bars) perifosine for 48 hours in the presence or absence of BMSCs. Cell proliferation was assessed by [<sup>3</sup>H]-thymidine uptake; data represent means ( $\pm$  SD) of quadruplicate cultures. (D) MM.1S cells were cultured with control media or perifosine (5  $\mu$ M) for 6 hours in the presence or absence of BMSCs. MM.1S cells were harvested, lysed, and subjected to Western blotting using anti-p-Akt, anti-Akt, anti-p-ERK, anti-ERK1/2, and p-STAT3 Abs.

STAT3; conversely, perifosine significantly inhibited IL-6-triggered Akt phosphorylation, without affecting ERK and STAT3 phosphorylation (Figure 3B). IGF-1-triggered Akt phosphorylation was similarly inhibited by perifosine. Since we have previously demonstrated that bortezomib down-regulates gp130 expression in a caspase-dependent manner and thereby inhibits IL-6-induced signaling cascades, including PI3-K/Akt, MEK/ERK, and Jak2/STAT3,<sup>42</sup> we similarly examined whether perifosine also triggers down-regulation of gp130 expression. perifosine did not trigger cleavage of either caspase-8 or PARP, confirming that inhibition of cytokine-mediated Akt phosphorylation by perifosine is not due to down-regulation of gp130 expression (data not shown). These results indicate that perifosine overcomes the antiapoptotic effect of IL-6 or IGF-1 and inhibits cytokine-stimulated Akt phosphorylation, without inhibiting ERK or STAT3.

Since the BM microenvironment confers MM cell growth and drug resistance,<sup>13,43,44</sup> we next studied whether perifosine inhibits MM cell growth in the context of the BM microenvironment. MM.1S cells were cultured with perifosine (2.5, 5, and 7.5  $\mu$ M), in the presence or absence of BMSCs. Adherence of MM.1S cells to BMSCs triggered increased [<sup>3</sup>H]-thymidine uptake (2.2-fold,  $P < .01$ ) (Figure 3C); conversely, perifosine inhibited this up-regulation in a dose-dependent fashion ( $P < .01$ ). The viability of BMSCs, assessed by MTT assay, was not inhibited by perifosine treatment (data not shown). Consistent with stimulation triggered by exogenous IL-6 (Figure 3B), adherence of MM.1S cells to BMSCs triggered phosphorylation of Akt, ERK, and STAT3; conversely, perifosine abrogated adherence-induced phosphorylation of Akt, without altering of ERK or STAT3 phosphorylation (Figure 3D). These data indicate that perifosine triggers significant antitumor activity even against MM cells in the BM milieu, associated with significant inhibition of Akt activity.

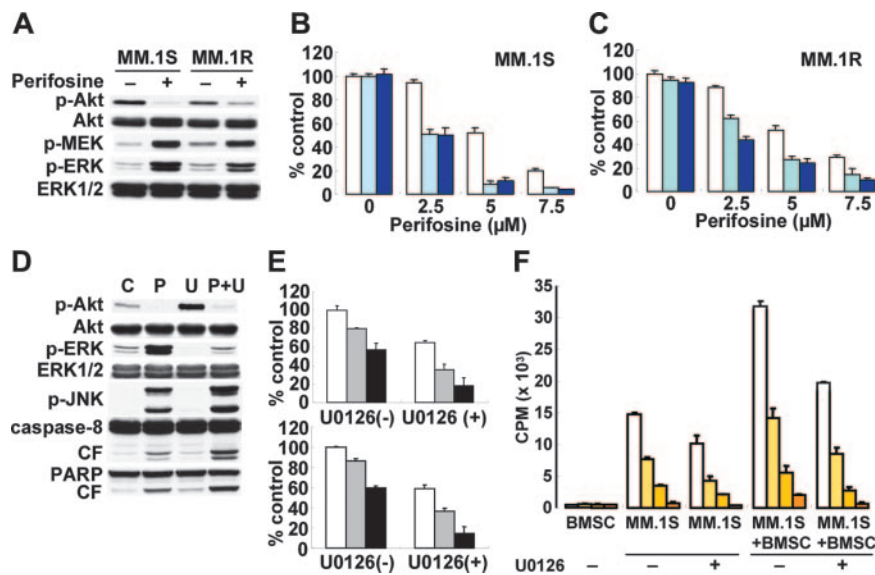


**Figure 4. Inhibition of ERK signaling augments Perifosine-induced cytotoxicity.** (A) MM.1S and MM.1R cells were cultured with perifosine (5  $\mu$ M) for 6 hours. Whole-cell lysates were subjected to Western blotting using anti-p-Akt, anti-Akt, anti-p-MEK, anti-p-ERK, and anti-ERK1/2 Abs. (B-C) MM.1S (B) and MM.1R (C) cells were cultured for 14 hours with control media and with 2.5  $\mu$ M, 5  $\mu$ M, and 7.5  $\mu$ M perifosine in the absence ( $\square$ ) or presence of 5  $\mu$ M (light blue bars) or 10  $\mu$ M (dark blue bars) MEK1/2 inhibitor U0126. Cytotoxicity was assessed by MTT assay; data represent means ( $\pm$  SD) of quadruplicate cultures. (D) MM.1S cells were cultured for 8 hours with control media, perifosine (5  $\mu$ M), U0126 (5  $\mu$ M), or perifosine (5  $\mu$ M) plus U0126 (5  $\mu$ M). Cells were then lysed and subjected to Western blotting using anti-p-Akt, anti-Akt, anti-p-ERK, anti-ERK1/2, anti-p-JNK, caspase-8, and PARP Abs. (E) Freshly isolated tumor cells from MM patients (n = 2) were cultured for 24 hours with control media ( $\square$ ) and with 5  $\mu$ M ( $\square$ ) or 10  $\mu$ M ( $\blacksquare$ ) perifosine in the presence or absence of U0126 (5  $\mu$ M). Cytotoxicity was assessed by MTT assay; data represent means ( $\pm$  SD) of quadruplicate cultures. (F) MM.1S cells were cultured for 48 hours with control media ( $\square$ ) and with 1.25  $\mu$ M (light orange bars), 2.5  $\mu$ M (medium orange bars), or 5  $\mu$ M (dark orange bars) perifosine with or without U0126 (2.5  $\mu$ M) and in the presence or absence of BMSCs. Cell proliferation was assessed by [ $^3$ H]-thymidine uptake; data represent means ( $\pm$  SD) of quadruplicate cultures.

#### Inhibition of ERK signaling synergistically augments perifosine-induced cytotoxicity

We have previously demonstrated an important role of MEK/ERK signaling in mediating proliferation in MM cells<sup>25,45</sup> as well as cross-talk between PI3-K/Akt and MEK/ERK signaling cascades.<sup>11</sup> Since perifosine triggered significant up-regulation of MEK and ERK phosphorylation, we hypothesized that this up-regulation might be a compensatory positive feedback response to maintain MM cell survival. Inhibiting MEK/ERK signaling would therefore enhance perifosine-induced cytotoxicity in MM cells. To inhibit up-regulation of MEK/ERK activity triggered by perifosine, we used the MEK1/2 inhibitor U0126. As seen in Figure 4A, Perifosine (5  $\mu$ M for 6 hours) markedly up-regulated phosphorylation of MEK and ERK in both MM.1S and MM.1R cells. As expected, the cytotoxicity triggered by perifosine was synergistically enhanced in the presence of U0126, determined by isobologram analysis: for example, 2.5  $\mu$ M and 5  $\mu$ M of perifosine alone induced 4% and 38% MM.1S cytotoxicity, which is increased to 50% (CI = 0.29) and 92% (CI = 0.37), respectively, by 5  $\mu$ M U0126 (Figure 4B). Similar results (CI = 0.43-0.58) were observed in MM.1R cells (Figure 4C).

The molecular mechanisms whereby perifosine-induced cytotoxicity is enhanced by U0126 were further studied. MM.1S cells were treated for 24 hours with 5  $\mu$ M perifosine, 5  $\mu$ M U0126, or the combination. Up-regulation of ERK phosphorylation triggered by perifosine was completely blocked by U0126 (Figure 4D). Importantly, phosphorylation of JNK and cleavage of caspase-8/PARP were markedly up-regulated by the combination versus single-agent treatment. Since we showed that JNK plays a crucial role in perifosine-induced cytotoxicity (Figure 2D-E), these results strongly suggest that augmentation of perifosine-induced cytotoxicity by U0126 is mediated via JNK activity, followed by caspase activation. We further examined whether this combination treatment was also effective in freshly isolated patient MM cells. Although perifosine alone was effective, U0126 (5  $\mu$ M) significantly augmented its cytotoxicity in patient tumor cells (Figure 4E). Importantly, no significant cytotoxicity in PBMCs was observed after perifosine and U0126 treatment (data not shown).

The combination of perifosine with U0126 was also examined in the context of MM cells bound to BMSCs. Either perifosine or

U0126 alone inhibited [ $^3$ H]-thymidine uptake triggered by adherence of MM.1S cells to BMSCs; importantly, U0126 (2.5  $\mu$ M) significantly enhanced perifosine-induced inhibition of [ $^3$ H]-thymidine uptake in adherent MM.1S cells (Figure 4F). The viability of BMSCs, assessed by MTT assay, was not altered by this combination treatment (data not shown). These data indicate that combined treatment of U0126 with perifosine triggers synergistic selective antitumor activity against MM cells in the BM milieu, thereby overcoming cell adhesion-mediated resistance to conventional therapies.

#### Perifosine enhances cytotoxicity of conventional (Dex, Mel, Dox) agents

Since Akt plays a crucial role mediating MM cell survival and antiapoptosis,<sup>10-12,46,47</sup> we hypothesized that inhibition of Akt activity by perifosine could enhance cytotoxicity of the conventional therapeutic agents Dex, Mel, and Dox. MM.1S cells were cultured for 48 hours with Dex (Figure 5A), Mel (Figure 5B), or Dox (Figure 5C), in the presence (2.5  $\mu$ M and 5  $\mu$ M) or absence of perifosine. Perifosine enhanced cytotoxicity triggered by these agents in a dose-dependent fashion. For example, 50 nM Dox induced 35% cytotoxicity, which was augmented to 60% and 86% by 2.5  $\mu$ M and 5  $\mu$ M perifosine, respectively (Figure 5C).

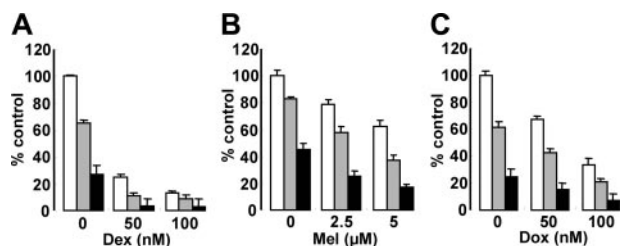


**Figure 5. Perifosine enhances cytotoxicity of conventional (Dex, Mel, Dox) agents.** MM.1S cells were cultured for 12 hours with control medium ( $\square$ ) and with 2.5  $\mu$ M (light bars) or 5  $\mu$ M (dark bars) perifosine in the presence or absence of (A) Dex, 50 nm and 100 nm; (B) Mel, 2.5  $\mu$ M and 5  $\mu$ M; and (C) Dox, 50 nm and 100 nm. Cytotoxicity was assessed by MTT assay; data represent the mean plus or minus SD of quadruplicate cultures.

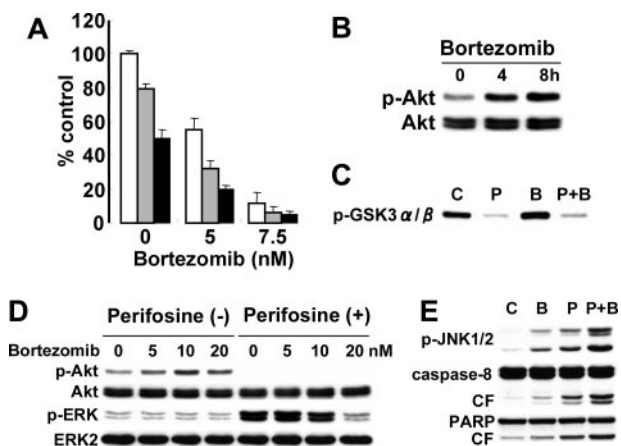


**Figure 6. Perifosine enhances cytotoxicity of novel (bortezomib) agents.** (A) MM.1S cells were cultured for 24 hours with control media (□) and with 2.5 μM (▨) or 5 μM (■) perifosine in the presence or absence of bortezomib (5 nM and 7.5 nM). Cytotoxicity was assessed by MTT assay; data represent means (± SD) of quadruplicate cultures. (B) MM.1S cells were cultured with bortezomib (10 nM) for 4 hours and 8 hours. Whole-cell lysates were subjected to Western blotting with p-Akt and Akt Abs. (C) MM.1S cells were cultured with bortezomib (10 nM) for 8 hours. Whole-cell lysates were immunoprecipitated with anti-Akt Ab. The immunoprecipitates were washed and subjected to in vitro kinase assay, according to manufacturer's protocol. The reaction mixtures were immunoblotted with anti-p-GSK3α/β. (D) MM.1S cells were cultured with bortezomib (5, 10, and 20 nM) in the presence (5 μM) or absence of perifosine. Whole-cell lysates were subjected to Western blotting with p-Akt, Akt, p-ERK, and ERK2 Abs. (E) MM.1S cells were cultured for 8 hours with control media, perifosine (5 μM), bortezomib (10 nM), or perifosine (5 μM) plus Bortezomib (10 nM). Cells were then lysed and subjected to Western blotting using anti-p-JNK1/2, caspase-8, and PARP Abs.

**Perifosine enhances cytotoxicity of a novel (bortezomib) agent**

Bortezomib demonstrates significant anti-MM activity in vitro,<sup>21,30,48</sup> in murine models of human MM in vivo,<sup>49</sup> and as therapy for patients with relapsed and refractory MM<sup>50,51</sup>; however, 60% to 65% of these patients did not respond to bortezomib. We therefore further examined whether perifosine could enhance the cytotoxicity of bortezomib. As expected, MM.1S cytotoxicity induced by bortezomib (5 and 7.5 nM) was significantly enhanced in the presence of perifosine (2.5 and 5 μM) (Figure 6A). We next analyzed the molecular mechanisms whereby perifosine enhanced bortezomib-triggered cytotoxicity. Surprisingly, bortezomib induced phosphorylation of Akt in a time-dependent fashion (Figure 6B). Augmentation of Akt kinase activity triggered by bortezomib was

confirmed using an in vitro Akt kinase assay (Figure 6C). Importantly, perifosine completely blocked bortezomib-triggered Akt activation.

Since we have previously shown that bortezomib inhibits ERK phosphorylation in MM.1S cells,<sup>21</sup> we further examined whether bortezomib blocks perifosine-induced phosphorylation of ERK. As shown in Figure 6D, perifosine-induced phosphorylation of ERK was inhibited by bortezomib in a dose-dependent fashion. We next treated MM.1S cells for 8 hours with 10 nM bortezomib, 5 μM perifosine, or the combination. Importantly, phosphorylation of JNK and cleavage of caspase-8/PARP were upregulated by the combination versus single agent treatment (Figure 6E). These results are similar to the combination treatment of perifosine with U0126, suggesting that opposing effects of bortezomib versus perifosine on phosphorylation of Akt and ERK, at least in part, modulate JNK/caspase activation.

**Perifosine inhibits human MM cell growth in vivo**

Having shown the signaling mechanisms mediating the anti-MM effects of perifosine in vitro, we next determined whether Perifosine mediates in vivo anti-human MM cell activity using an immunodeficient murine plasmacytoma model. In a 4-week treatment toxicity study, the maximum tolerated dose was determined as 250 mg/kg/wk in 2 divided doses or 36 mg/kg/d as a single dose. These doses were therefore used to assess antimyeloma activity.

Mice were inoculated subcutaneously in the flank with 3 × 10<sup>7</sup> MM.1S MM cells in 100 μL RPMI-1640 media, together with 100 μL Matrigel. Drug treatment was started after the development of measurable tumor. Perifosine was given via oral gavage at doses of 250 mg/kg/wk in 2 divided doses or 36 mg/kg/d. Control mice were given PBS vehicle only. Serial caliper measurements of perpendicular diameters were done every other day to calculate tumor volume. There was no significant difference between the groups at baseline (P = .8).

Both oral daily (36 mg/kg/d) and weekly (250 mg/kg/wk) administration of perifosine significantly reduced MM tumor growth and increased survival, compared with control animals treated with PBS vehicle only. Comparisons of tumor volumes on day 15 following tumor implantation showed statistically significant differences across treatment groups (P = .016, 1-way analysis of variance), and Bonferroni post hoc tests revealed significantly lower tumor volumes in both the perifosine-treated groups versus the control group (P = .04; Figure 7A). In contrast, there was no

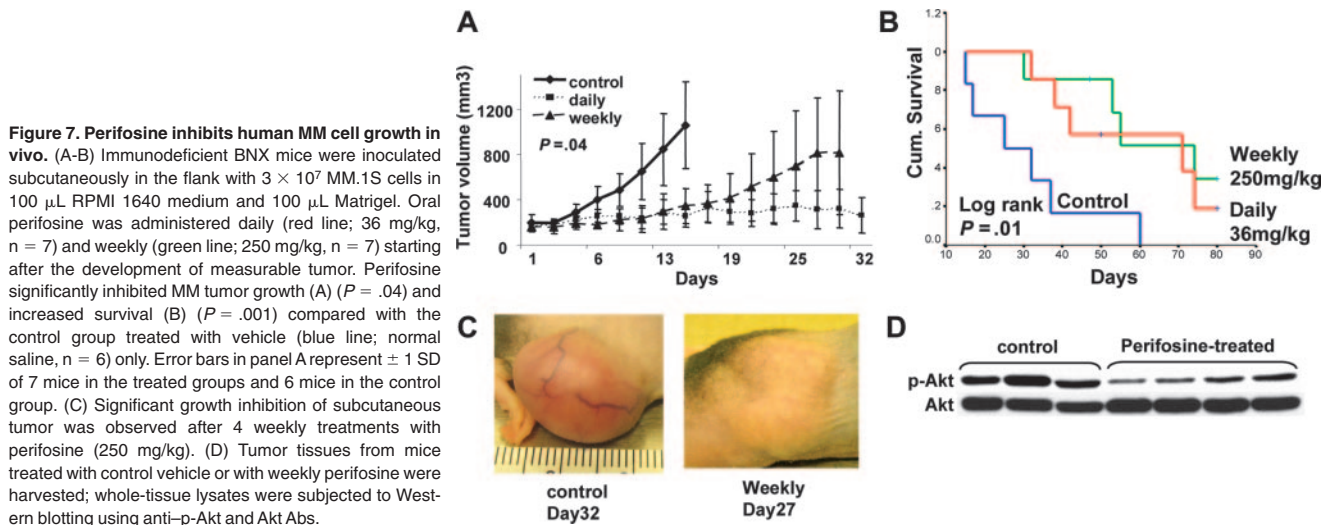


**Figure 7. Perifosine inhibits human MM cell growth in vivo.** (A-B) Immunodeficient BNX mice were inoculated subcutaneously in the flank with 3 × 10<sup>7</sup> MM.1S cells in 100 μL RPMI 1640 medium and 100 μL Matrigel. Oral perifosine was administered daily (red line; 36 mg/kg, n = 7) and weekly (green line; 250 mg/kg, n = 7) starting after the development of measurable tumor. Perifosine significantly inhibited MM tumor growth (A) (P = .04) and increased survival (B) (P = .001) compared with the control group treated with vehicle (blue line; normal saline, n = 6) only. Error bars in panel A represent ± 1 SD of 7 mice in the treated groups and 6 mice in the control group. (C) Significant growth inhibition of subcutaneous tumor was observed after 4 weekly treatments with perifosine (250 mg/kg). (D) Tumor tissues from mice treated with control vehicle or with weekly perifosine were harvested; whole-tissue lysates were subjected to Western blotting using anti-p-Akt and Akt Abs.

significant difference between the perifosine treatment groups. Assessing overall survival (OS), all control mice were killed by day 60 after treatment was begun, whereas 71% of daily treated mice and 57% of weekly treated mice remained alive at this time. Using Kaplan-Meier curves and log-rank analysis, the mean OS was 31 days (95% confidence interval [CI], 18-44 days) in the control cohort versus 59 days (95% CI, 45-73 days) and 63 days (95% CI, 49-76 days) in groups treated with daily and weekly perifosine, respectively. There was no statistically significant difference in the mean OS of mice treated with the 2 doses of perifosine. In contrast, a statistically significant prolongation in mean OS compared with control mice was observed in animals treated with daily ( $P = .011$ ) and weekly ( $P = .016$ ) perifosine (Figure 7B). Furthermore, these results underestimate the survival advantage of perifosine to these mice because 5 (36%) of treated mice were killed on day 81 in order to further examine molecular events *ex vivo*. These mice either had no tumor (1) or small tumors well controlled by the drug (4).

Some toxicity was observed in the treated group. During the first 35 days, there was a nonsignificant weight loss of 6% to 9% in the treated groups compared with controls. Significant weight loss was observed in 3 treated mice, but this occurred after 5 weeks of treatment when most of the control mice had already been killed. It is therefore not certain that the morbidity was drug related. Histologic examination of organs did not reveal any organ toxicity, and the causes of the morbidity were not clear. Representative significant inhibition of tumor growth by weekly perifosine is shown in Figure 7C. Whole-tumor-cell lysates from vehicle control and weekly perifosine-treated mice were subjected to Western blotting to assess *in vivo* phosphorylation of Akt. Importantly, tumor tissue from perifosine-treated mice demonstrated significant inhibition of Akt phosphorylation compared with tumor tissue from control animals (Figure 7D). Evaluation of terminal bleeds did not reveal any differences in hematologic parameters in drug treated versus control mice (data not shown).

## Discussion

In the BM microenvironment, the interaction of MM cells with BMSCs triggers activation of MEK/ERK, JAK2/STAT3, and PI3-K/Akt signaling cascades, which induce MM cell proliferation, survival, drug resistance, and migration.<sup>13,14,43</sup> Among these signaling cascades, PI3-K/Akt has been demonstrated to have the most significant biologic impact in MM cell-cycle regulation and antiapoptosis.<sup>10,11,52-56</sup> In the context of BMSCs, PI3-K/Akt is activated by various cytokines, including IL-6,<sup>11</sup> IGF-1,<sup>10,12</sup> VEGF,<sup>56</sup> stromal cell-derived factor 1 $\alpha$  (SDF-1 $\alpha$ ),<sup>52</sup> and macrophage inflammatory protein 1- $\alpha$ .<sup>57</sup> Specifically, Dex-induced apoptosis is significantly inhibited by IL-6 and IGF-1 via activation of the PI3-K/Akt pathway. Most recently, B-cell-activating factor has similarly been reported to abrogate Dex-induced apoptosis in MM.<sup>53,58</sup>

Perifosine is an alkylphospholipid, a novel class of antitumor agents structurally related to ether lipids that interacts with the cell membrane and thereby modulates intracellular growth signal transduction pathways. In preclinical studies, perifosine blocks cell-cycle progression in head and neck squamous cell carcinoma by inducing p21<sup>WAF1</sup>, regardless of p53 function.<sup>17</sup> Importantly, perifosine inhibits Akt/protein kinase B (PKB) activity, associated with activation of the stress-activated protein kinase (SAPK)/JNK pathway,<sup>16</sup> without affecting PI3-K or PDK-1 activity.<sup>15</sup> Two phase 1 studies of perifosine in advanced solid tumors have already been

reported<sup>20,59</sup>; no hematology toxicity was observed. Since Akt plays a crucial role in MM cell survival and antiapoptosis, we in this study hypothesized that inhibition of Akt activity by perifosine could represent a novel therapeutic strategy in MM.

Although we observed constitutive phosphorylation of Akt to be variable in cell lines, the majority shows both Ser473 and Thr308 phosphorylation. There is no specific relationship between baseline expression of p-Akt, pSTAT3, and p-ERK. Perifosine, in a time- and dose-dependent fashion, significantly inhibits constitutive phosphorylation of Akt and its downstream molecules FKHL1 and GSK3 $\alpha/\beta$ , which play important roles in cell cycle and survival in MM.1S cells. Importantly, it does not alter the phosphorylation of upstream PDK-1. These results are consistent with a previous report,<sup>15</sup> and suggest that perifosine directly blocks Akt activity. Interestingly, perifosine enhances phosphorylation of MEK and ERK in a time- and dose-dependent fashion. Since the MEK/ERK pathway mediates MM cell proliferation,<sup>25,45</sup> perifosine-induced MEK/ERK phosphorylation may be a compensatory mechanism in MM cells. Cytotoxicity triggered by perifosine is significant in all MM cell lines, including Dex-resistant (MM.1R), Mel-resistant (RPMI-LR5), and Dox-resistant (RPMI-Dox-40) cells, with IC<sub>50</sub> at 48 hours of 1 to 20  $\mu$ M, suggesting that perifosine overcomes resistance to conventional agents. Importantly, perifosine also induces cytotoxicity in freshly isolated tumor cells from patients with MM in this range of IC<sub>50</sub>, without cytotoxicity in PBMCs. Importantly, perifosine is also active in Myr-Akt transfected cells, suggesting that perifosine overcomes hyperactive Akt.

Perifosine triggers JNK phosphorylation in a time- and dose-dependent fashion in MM cells, consistent with previous reports.<sup>16,60</sup> Since we have shown that JNK plays a crucial role in apoptosis induced by bortezomib<sup>30</sup> and lysophosphatidic acid acyltransferase inhibitor,<sup>34</sup> we next determined the role of JNK activity mediating perifosine-induced apoptosis. As expected, JNK inhibitor SP600125 almost completely blocks caspase-8 cleavage and cytotoxicity. This result is further confirmed by down-regulation of JNK2 by transfection of JNK2 siRNA. Taken together, these results indicate that JNK plays an obligate role in perifosine-induced apoptosis in MM cells. p38 MAPK is also phosphorylated by perifosine treatment, and blockade of p38 MAPK using the specific inhibitor SCIO469 significantly enhanced perifosine-induced cytotoxicity. Since our previous studies have shown that inhibition of p38 MAPK augments bortezomib-triggered cytotoxicity via down-regulation of heat shock protein (Hsp) 27,<sup>31</sup> these results suggest that expression and/or activation of Hsp27 may be associated with perifosine-induced cytotoxicity.

We and others have shown that IL-6 abrogates Dex-induced MM cell apoptosis via activation of Akt,<sup>10,11</sup> and therefore further examined whether IL-6 or MM cell adherence to BMSCs could block perifosine-induced apoptosis in MM. perifosine triggers cytotoxicity even in the presence of IL-6 and in MM cells adherent to BMSCs, suggesting that perifosine can overcome CAM-DR in the BM milieu.

Since ERK is activated by perifosine treatment and plays a crucial role in MM cell proliferation, we hypothesized that inhibition of ERK activity would augment perifosine-induced cytotoxicity in MM cell lines and patient MM cells. As expected, MEK inhibitor U0126 synergistically enhances perifosine-induced cytotoxicity, associated with augmentation of JNK phosphorylation and caspase-8/PARP cleavage, confirming that dual inhibition of Akt and MEK/ERK induces synergistic antitumor activity in MM



cells. Most recently, Rahmani et al have reported that coadministration of HDAC inhibitors with perifosine in human leukemia cells leads to inhibition of both Akt and MEK/ERK, as well as a marked increase in apoptosis.<sup>19</sup> Dasmahapatra et al have also reported that UCN-01, which inhibits PDK-1, together with perifosine, induces synergistic inhibition of prostate and lung cancer cell line growth at clinically achievable doses and without toxicity.<sup>33</sup> In this study, we combined perifosine with conventional anti-MM agents (Dex, Mel, Dox) and demonstrated enhanced cytotoxicity, suggesting potential clinical activity of combination therapies.

The proteasome inhibitor bortezomib induces significant antitumor activity in human MM cell lines and patient MM cells associated with JNK/caspase activation and followed by apoptosis, even in the presence of BMSCs.<sup>13,21,29,30,42,48,61</sup> Importantly, phase 2 and 3 trials of bortezomib treatment of patients with refractory and/or relapsed MM demonstrated responses; however, some patients did not respond and others acquired resistance.<sup>50,51</sup> We have recently demonstrated that inhibition of the aggresome, an

alternative pathway for degradation of polyubiquitinated proteins, using the specific HDAC6 inhibitor tubacin can synergistically augment bortezomib-induced cytotoxicity.<sup>32</sup> Interestingly, the present studies showed that bortezomib triggers activation of Akt, which is completely blocked by perifosine; conversely, perifosine-induced ERK phosphorylation is inhibited by bortezomib. This blockade by perifosine and bortezomib of both Akt and ERK signaling cascades enhances JNK phosphorylation, caspase/PARP cleavage, and apoptosis, suggesting promise of this combination to overcome clinical proteasome resistance.

Finally, perifosine is well tolerated and very effective in vivo in a murine MM model, evidenced by significant inhibition of MM tumor growth in mice treated with either daily (36 mg/kg) or weekly (250 mg/kg) oral perifosine, associated with Akt inhibition in tumor cells. These results, coupled with its lack of toxicity in these preclinical mouse models, provide the framework for clinical studies of perifosine, alone and coupled with conventional and proteasome inhibitor therapies, to improve patient outcome in MM.

## References

- Gregory WM, Richards MA, Malpas JS. Combination chemotherapy versus melphalan and prednisolone in the treatment of multiple myeloma: an overview of published trials. *J Clin Oncol*. 1992;10:334-342.
- Myeloma Trialists' Collaborative Group. Combination chemotherapy versus melphalan plus prednisone as treatment for multiple myeloma: an overview of 6,633 patients from 27 randomized trials. *J Clin Oncol*. 1998;16:3832-3842.
- Lenhoff S, Hjorth M, Holmberg E, et al. Impact on survival of high-dose therapy with autologous stem cell support in patients younger than 60 years with newly diagnosed multiple myeloma: a population-based study. *Blood*. 2000;95:7-11.
- Attal M, Harousseau JL, Facon T, et al. Single versus double autologous stem-cell transplantation for multiple myeloma. *N Engl J Med*. 2003;349:2495-2502.
- Sonneveld P. Drug resistance in myeloma. *Pathol Biol (Paris)*. 1999;47:182-187.
- Covelli A. Modulation of multidrug resistance (MDR) in hematological malignancies. *Ann Oncol*. 1999;10:53-59.
- Schwarzenbach H. Expression of MDR1/P-glycoprotein, the multidrug resistance protein MRP, and the lung-resistance protein LRP in multiple myeloma. *Med Oncol*. 2002;19:87-104.
- Damiano JS, Cress AE, Hazlehurst LA, Shtil AA, Dalton WS. Cell adhesion mediated drug resistance (CAM-DR): role of integrins and resistance to apoptosis in human myeloma cell lines. *Blood*. 1999;93:1658-1667.
- Hazlehurst LA, Damiano JS, Buyuksal I, Pledger WJ, Dalton WS. Adhesion to fibronectin via beta1 integrins regulates p27<sup>kip1</sup> levels and contributes to cell adhesion mediated drug resistance (CAM-DR). *Oncogene*. 2000;19:4319-4327.
- Tu Y, Gardner A, Lichtenstein A. The phosphatidylinositol 3-kinase/Akt kinase pathway in multiple myeloma plasma cells: roles in cytokine-dependent survival and proliferative responses. *Cancer Res*. 2000;60:6763-6770.
- Hideshima T, Nakamura N, Chauhan D, Anderson KC. Biologic sequelae of interleukin-6 induced PI3-K/Akt signaling in multiple myeloma. *Oncogene*. 2001;20:5991-6000.
- Mitsiades CS, Mitsiades N, Poulaki V, et al. Activation of NF- $\kappa$ B and upregulation of intracellular anti-apoptotic proteins via the IGF-1/Akt signaling in human multiple myeloma cells: therapeutic implications. *Oncogene*. 2002;21:5673-5683.
- Hideshima T, Anderson KC. Molecular mechanisms of novel therapeutic approaches for multiple myeloma. *Nat Rev Cancer*. 2002;2:927-937.
- Hideshima T, Bergsagel PL, Kuehl WM, Anderson KC. Advances in biology of multiple myeloma: clinical applications. *Blood*. 2004;104:607-618.
- Kondapaka SB, Singh SS, Dasmahapatra GP, Sausville EA, Roy KK. Perifosine, a novel alkylphospholipid, inhibits protein kinase B activation. *Mol Cancer Ther*. 2003;2:1093-1103.
- Ruiter GA, Zerp SF, Bartelink H, van Blitterswijk WJ, Verheij M. Anti-cancer alkyl-lysophospholipids inhibit the phosphatidylinositol 3-kinase-Akt/PKB survival pathway. *Anticancer Drugs*. 2003;14:167-173.
- Patel V, Lahusen T, Sy T, Sausville EA, Gutkind JS, Senderowicz AM. Perifosine, a novel alkylphospholipid, induces p21<sup>WAF1</sup> expression in squamous carcinoma cells through a p53-independent pathway, leading to loss in cyclin-dependent kinase activity and cell cycle arrest. *Cancer Res*. 2002;62:1401-1409.
- De Siervi A, Marinissen M, Diggs J, Wang XF, Pages G, Senderowicz A. Transcriptional activation of p21<sup>WAF1/cip1</sup> by alkylphospholipids: role of the mitogen-activated protein kinase pathway in the transactivation of the human p21<sup>WAF1/cip1</sup> promoter by Sp1. *Cancer Res*. 2004;64:743-750.
- Rahmani M, Reese E, Dai Y, et al. Coadministration of histone deacetylase inhibitors and perifosine synergistically induces apoptosis in human leukemia cells through Akt and ERK1/2 inactivation and the generation of ceramide and reactive oxygen species. *Cancer Res*. 2005;65:2422-2432.
- Crul M, Rosing H, de Klerk GJ, et al. Phase I and pharmacological study of daily oral administration of perifosine (D-21266) in patients with advanced solid tumours. *Eur J Cancer*. 2002;38:1615-1621.
- Hideshima T, Richardson P, Chauhan D, et al. The proteasome inhibitor PS-341 inhibits growth, induces apoptosis, and overcomes drug resistance in human multiple myeloma cells. *Cancer Res*. 2001;61:3071-3076.
- Hideshima T, Chauhan D, Shima Y, et al. Thalidomide and its analogues overcome drug resistance of human multiple myeloma cells to conventional therapy. *Blood*. 2000;96:2943-2950.
- Klein B. Cytokine, cytokine receptors, transduction signals, and oncogenes in human multiple myeloma. *Semin Hematol*. 1995;32:4-19.
- Lichtenstein A, Tu Y, Fady C, Vescio R, Berenson J. Interleukin-6 inhibits apoptosis of malignant plasma cells. *Cell Immunol*. 1995;162:248-255.
- Ogata A, Chauhan D, Teoh G, et al. Interleukin-6 triggers cell growth via the *ras*-dependent mitogen-activated protein kinase cascade. *J Immunol*. 1997;159:2212-2221.
- Chauhan D, Kharbada S, Ogata A, et al. Interleukin-6 inhibits Fas-induced apoptosis and stress-activated protein kinase activation in multiple myeloma cells. *Blood*. 1997;89:227-234.
- Freund GG, Kulas DT, Mooney RA. Insulin and IGF-1 increase mitogenesis and glucose metabolism in the multiple myeloma cell line, RPM1 8226. *J Immunol*. 1993;151:1811-1820.
- Mitsiades CS, Mitsiades NS, McMullan CJ, et al. Inhibition of the insulin-like growth factor receptor-1 tyrosine kinase activity as a therapeutic strategy for multiple myeloma, other hematologic malignancies, and solid tumors. *Cancer Cell*. 2004;5:221-230.
- Hideshima T, Chauhan D, Richardson P, et al. NF- $\kappa$ B as a therapeutic target in multiple myeloma. *J Biol Chem*. 2002;277:16639-16647.
- Hideshima T, Mitsiades C, Akiyama M, et al. Molecular mechanisms mediating antimyeloma activity of proteasome inhibitor PS-341. *Blood*. 2003;101:1530-1534.
- Hideshima T, Podar K, Chauhan D, et al. p38 MAPK inhibition enhances PS-341 (bortezomib)-induced cytotoxicity against multiple myeloma cells. *Oncogene*. 2004;23:8766-8776.
- Hideshima H, Bradner JE, Wong J, et al. Small molecule inhibition of proteasome and aggresome function induces synergistic anti-tumor activity in multiple myeloma. *Proc Natl Acad Sci USA*. 2005;102:8567-8572.
- Dasmahapatra GP, Didolkar P, Alley MC, Ghosh S, Sausville EA, Roy KK. In vitro combination treatment with perifosine and UCN-01 demonstrates synergism against prostate (PC-3) and lung (A549) epithelial adenocarcinoma cell lines. *Clin Cancer Res*. 2004;10:5242-5252.
- Hideshima T, Chauhan D, Hayashi T, et al. Anti-tumor activity of lysophosphatidic acid acyltransferase (LPAAT)- $\beta$ inhibitors, a novel class of agents, in multiple myeloma. *Cancer Res*. 2003;63:8428-8436.
- Bennett BL, Sasaki DT, Murray BW, et al. SP600125, an anthranyprazolone inhibitor of Jun N-terminal kinase. *Proc Natl Acad Sci U S A*. 2001;98:13681-13686.
- Han Z, Boyle DL, Chang L, et al. c-Jun N-terminal kinase is required for metalloproteinase expression and joint destruction in inflammatory arthritis. *J Clin Invest*. 2001;108:73-81.
- Hochedlinger K, Wagner EF, Sabapathy K. Differential effects of JNK1 and JNK2 on signal specific

- induction of apoptosis. *Oncogene*. 2002;21:2441-2445.
38. Kawano M, Hirano T, Matsuda T, et al. Autocrine generation and requirement of BSF-2/IL-6 for human multiple myelomas. *Nature*. 1988;332:83-85.
  39. Klein B, Zhang XG, Jourdan M, et al. Paracrine rather than autocrine regulation of myeloma-cell growth and differentiation by interleukin-6. *Blood*. 1989;73:517-526.
  40. Tassone P, Neri P, Burger R, et al. Combination therapy with IL-6 receptor super-antagonist Sant7 and dexamethasone induces antitumor effects in a novel SCID-hu in vivo model of human multiple myeloma. *Clin Cancer Res*. 2005;11:4251-4258.
  41. Tassone P, Neri P, Carrasco DR, et al. A clinically relevant SCID-hu in vivo model of human multiple myeloma. *Blood*. 2005;106:713-716.
  42. Hideshima T, Chauhan D, Hayashi T, et al. Proteasome inhibitor PS-341 abrogates IL-6 triggered signaling cascades via caspase-dependent downregulation of gp130 in multiple myeloma. *Oncogene*. 2003;22:8386-8393.
  43. Hideshima T, Richardson P, Anderson KC. Novel therapeutic approaches for multiple myeloma. *Immunol Rev*. 2003;194:164-176.
  44. Mitsiades CS, Mitsiades N, Munshi NC, Anderson KC. Focus on multiple myeloma. *Cancer Cell*. 2004;6:439-444.
  45. Ogata A, Chauhan D, Urashima M, Teoh G, Treon SP, Anderson KC. Blockade of mitogen-activated protein kinase cascade signaling in interleukin-6 independent multiple myeloma cells. *Clin Cancer Res*. 1997;3:1017-1022.
  46. Hsu J, Shi Y, Krajewski S, et al. The AKT kinase is activated in multiple myeloma tumor cells. *Blood*. 2001;98:2853-2855.
  47. Hsu JH, Shi Y, Hu L, Fisher M, Franke TF, Lichtenstein A. Role of the AKT kinase in expansion of multiple myeloma clones: effects on cytokine-dependent proliferative and survival responses. *Oncogene*. 2002;21:1391-1400.
  48. Mitsiades N, Mitsiades CS, Poulaki V, et al. Molecular sequelae of proteasome inhibition in human multiple myeloma cells. *Proc Natl Acad Sci U S A*. 2002;99:14374-14379.
  49. LeBlanc R, Catley LP, Hideshima T, et al. Proteasome inhibitor PS-341 inhibits human myeloma cell growth in vivo and prolongs survival in a murine model. *Cancer Res*. 2002;62:4996-5000.
  50. Richardson PG, Barlogie B, Berenson J, et al. A phase 2 study of bortezomib in relapsed, refractory myeloma. *N Engl J Med*. 2003;348:2609-2617.
  51. Richardson PG, Sonneveld P, Schuster MW, et al. Bortezomib or high-dose dexamethasone for relapsed multiple myeloma. *N Engl J Med*. 2005;352:2487-2498.
  52. Hideshima T, Chauhan D, Hayashi T, et al. The biological sequelae of stromal cell-derived factor-1alpha in multiple myeloma. *Mol Cancer Ther*. 2002;1:539-544.
  53. Klein B, Tarte K, Jourdan M, et al. Survival and proliferation factors of normal and malignant plasma cells. *Int J Hematol*. 2003;78:106-113.
  54. Tai YT, Podar K, Catley L, et al. Insulin-like growth factor-1 induces adhesion and migration in human multiple myeloma cells via activation of beta1-integrin and phosphatidylinositol 3'-kinase/AKT signaling. *Cancer Res*. 2003;63:5850-5858.
  55. Lentzsch S, Chatterjee M, Gries M, et al. PI3-K/AKT/FKHR and MAPK signaling cascades are redundantly stimulated by a variety of cytokines and contribute independently to proliferation and survival of multiple myeloma cells. *Leukemia*. 2004;18:1883-1890.
  56. Podar K, Anderson KC. The pathophysiological role of VEGF in hematological malignancies: therapeutic implications. *Blood*. 2005;105:1383-1395.
  57. Lentzsch S, Gries M, Janz M, Bargou R, Dorken B, Mavrou M. Macrophage inflammatory protein 1-alpha (MIP-1 alpha) triggers migration and signaling cascades mediating survival and proliferation in multiple myeloma (MM) cells. *Blood*. 2003;101:3568-3573.
  58. Moreaux J, Legouffe E, Jourdan E, et al. BAFF and APRIL protect myeloma cells from apoptosis induced by interleukin 6 deprivation and dexamethasone. *Blood*. 2004;103:3148-3157.
  59. Van Ummersen L, Binger K, Volkman J, et al. A phase I trial of perifosine (NSC 639966) on a loading dose/maintenance dose schedule in patients with advanced cancer. *Clin Cancer Res*. 2004;10:7450-7456.
  60. Ruiters GA, Zerp SF, Bartelink H, van Blitterswijk WJ, Verheij M. Alkyl-lysophospholipids activate the SAPK/JNK pathway and enhance radiation-induced apoptosis. *Cancer Res*. 1999;59:2457-2463.
  61. Hideshima T, Chauhan D, Schlossman RL, Richardson PR, Anderson KC. Role of TNF- $\alpha$  in the pathophysiology of human multiple myeloma: therapeutic applications. *Oncogene*. 2001;20:4519-4527.